King's College London

Robot Dynamics & Control (7CCEMRDC)

Dynamical Modelling and Control of an Underactuated Articulated-Soft Robotic Manipulator

Coursework Report

Student Name: Naghim Ibragimov
Student ID: K22031784

Submission Date: 1 April 2026

1 Introduction

This coursework is about the modelling and control of a two degree of freedom (2-DoF) articulated soft robotic manipulator in a Drake simulation environment. The system consists of two links connected thorugh compliant joints, resulting in flexible joint dynamics and an underactuated structure, which makes control tougher than in rigid manipulators.

The task is to have the manipulator to interact with a wall located to its right. Specifically, the end-effector must reach the wall, establish stable contact, and execute a vertical motion while maintaining that contact. This task introduces a dual requirement: accurate trajectory tracking and controlled interaction with the environment.

Achieving both objectives simultaneously is not easy. Poor tracking performance leads to bad motion, while excessive contact forces can cause the wall to move and ruin the system. The controller must therefore balance motion accuracy and interaction forces, ensuring smooth behaviour during contact.

The objective of this report is to develop and evaluate a control strategy that enables stable trajectory tracking and interaction for the articulated-soft manipulator. The system dynamics are first shown, followed by the design of joint and Cartesian space controllers. The stability of the closed-loop system is then analysed, and the performance is evaluated through simulation results and robustness analysis.

2 System Modelling

2.1 System Description

The system is a planar two degree of freedom (2-DoF) articulated soft robotic manipulator. It has two rigid links connected through compliant joints, where actuation is given by motors that are elastically coupled to the links. Therefore, the motor coordinates are not directly equal to the link coordinates, leading to flexible-joint dynamics.

Unlike conventional rigid manipulators, the presence of compliance introduces extra dynamic effects such as oscillations and delayed transmission of torque from the motors to the links. This significantly increases the difficulty of the system and must be accounted for in the control design.

The manipulator operates in a vertical plane and is subject to gravitational forces. The end effector interacts with a moving wall located to the right of the robot, introducing contact forces into the system and creating a tougher problem.

2.2 Underactuation and Compliance

The system is classified as underactuated, as the number of independent state variables exceeds the number of available control inputs. In this case, the motors act on internal coordinates, and the link motion is achieved indirectly through elastic elements. Consequently, the control inputs do not directly command the link positions, but instead influence them via spring deflections.

This makes the control problem more challenging, particularly in the presence of extra contact, where precise regulation of both motion and interaction forces is required.

2.3 Environment and Interaction

In addition to free space motion, the manipulator must interact with a wall. The wall is able to translate when subjected to force, meaning that to much force from the manipulator will result in wall movement.

This introduces an important requirement for the control system: the manipulator must maintain stable contact while minimising disturbance to the environment. As a result, the system must balance trajectory tracking accuracy with compliant interaction behaviour.

2.4 General Dynamic Behaviour

The dynamics of a robotic manipulator can be expressed in this form

$$M(q)\ddot{q} + C(q,\dot{q})\dot{q} + \tau_g(q) = \tau, \tag{1}$$

where $q \in \mathbb{R}^2$ represents the joint coordinates, $\dot{q}$ and $\ddot{q}$ denote joint velocities and accelerations, $M(q)$ is the inertia matrix, $C(q,\dot{q})$ captures the centrifugal effects, $\tau_g(q)$ represents gravitational torques, and τ is the vector of applied torques.

This shows nonlinear and coupled nature of the system dynamics. In the case of articulated-soft manipulators, these dynamics are further influenced by joint elasticity and damping, which introduce additional coupling between motor and link motion. These effects must be considered when developing a control strategy capable of achieving both accurate motion and stable interaction.

2.5 Flexible Joint Dynamics

In addition to the standard rigid-body dynamics, the articulated-soft manipulator is characterised by flexible joint behaviour. This introduces a coupling between motor coordinates θ and link coordinates q, resulting in the following dynamic model:

$$M(q)\ddot{q} + C(q,\dot{q})\dot{q} + K(q-\theta) + \tau_g(q) = 0, \tag{2}$$

$$J\ddot{\theta} + D\dot{\theta} + K(\theta - q) = \tau_m, \tag{3}$$

where θ represents the motor coordinates, K is the joint stiffness matrix, and D represents motor damping. The term $(q-\theta)$ corresponds to the spring deflection between motor and link positions.

This model highlights the indirect actuation of the links through elastic elements, which is the source of underactuation and additional dynamic difficulty.

3 Control Design

3.1 Control Architecture

The implemented controller combines task regulation, joint-space control, and flexible-joint damping to achieve stable trajectory tracking and compliant interaction with the environment. The control input is the motor torque $\tau_m \in \mathbb{R}^2$, which acts on the motor-side dynamics of the flexible-joint system.

The controller operates mainly in Cartesian space to regulate end-effector motion, while joint-space terms are used for trajectory mapping and stabilisation. Additional damping and practical constraints are incorporated to ensure robust behaviour during contact with the wall.

3.2 Reference Generation and Kinematics

A desired Cartesian trajectory $c_{\text{des}}(t) = [x_{\text{des}}, z_{\text{des}}]^T$ is specified. The corresponding end-effector position is computed using forward kinematics:

$$c = \begin{bmatrix} L_1 \cos(q_1) + L_2 \cos(q_1 + q_2) \\ L_1 \sin(q_1) + L_2 \sin(q_1 + q_2) \end{bmatrix}. \tag{4}$$

The Jacobian matrix $J(q)$ relates joint velocities to Cartesian velocity:

$$\dot{c} = J(q)\dot{q}. \tag{5}$$

For trajectory tracking, inverse kinematics is used to compute joint references q_{des} corresponding to c_{des}.

3.3 Joint-Space Regulation

Joint space control is used to track desired configurations and stable motion. A wrapped angle error is defined as:

$$e_{\text{wrap}} = \text{atan2}(\sin(q_{\text{des}} - q), \cos(q_{\text{des}} - q)), \tag{6}$$

which ensures continuing across angular discontinuities.

The joint space PD control law is:

$$\tau_{\text{PD}} = K_p e_{\text{wrap}} + K_d(\dot{q}_{\text{des}} - \dot{q}). \tag{7}$$

3.4 Task-Space Control and Impedance Behaviour

The primary control action is defined in task space through a virtual force acting on the end-effector:

$$F_{\text{virtual}} = K_d(c_{\text{des}} - c) + D_d(\dot{c}_{\text{des}} - \dot{c}), \tag{8}$$

where K_d and D_d are diagonal stiffness and damping matrices, allowing independent tuning in both directions.

This virtual force is mapped to joint torques using the Jacobian transpose:

$$\tau_{\text{task}} = J(q)^T F_{\text{virtual}}. \tag{9}$$

This produces compliant behaviour and is well suited for contact tasks, since there is no explicit inversion of the robot dynamics.

3.5 Flexible Joint Damping

To suppress oscillations arising from joint compliance, additional damping is applied on the motor and spring dynamics:

$$\tau_{\text{damp}} = -D_{\text{motor}}\dot{\theta} - D_\delta\dot{\delta}, \tag{10}$$

where $\delta = \theta - q$ is the spring deflection. These terms loose energy from motor-side motion and flexible-joint oscillations.

3.6 Gravity Compensation

Gravity effects are compensated using a model-based term:

$$\tau_g(q) = \begin{bmatrix} (m_1 + m_2)gL_1\sin(q_1) + m_2gL_2\sin(q_1 + q_2) \\ m_2gL_2\sin(q_1 + q_2) \end{bmatrix}. \tag{11}$$

3.7 Final Control Law

The commanded motor torque is given by:

$$\tau = \tau_{\text{task}} + \tau_g(q) - D_{\text{motor}}\dot{\theta} - D_\delta\dot{\delta}. \tag{12}$$

3.8 Practical Constraints and Contact Handling

To ensure stable and physically realistic behaviour, several practical constraints are applied:

- **Torque saturation**: limits actuator effort within allowable bounds.
- **Rate limiting**: prevents fast torque changes that excite flexible dynamics.
- **Low-pass filtering**: smooths high-frequency control signals.
- **Force clamping**: limits the commanded force in the wall-normal direction during contact.

These modifications are vital for achieving stable contact interaction and reducing oscillations in the flexible-joint system.

4 Kinematics and Task-Space Mapping

4.1 Forward Kinematics

The controller is formulated in Cartesian space, and therefore the end effector position must be taken from the link coordinates through FK. For the planar two-link manipulator considered in this coursework, the end effector position is given by

$$\begin{bmatrix} x \\ z \end{bmatrix} = \begin{bmatrix} L_1 \cos(q_1) + L_2 \cos(q_1 + q_2) \\ L_1 \sin(q_1) + L_2 \sin(q_1 + q_2) \end{bmatrix}, \tag{13}$$

where L_1 and L_2 denote the link lengths, and q_1, q_2 are the link angles. In the shown model, the kinematics are evaluated using the link side coordinates q, rather than the motor coordinates θ, since the compliant joints introduce a difference between motor motion and link motion.

4.2 Jacobian Matrix

The relationship between joint velocities and end-effector velocities is described by the manipulator Jacobian,

$$\dot{x} = J(q)\dot{q}, \tag{14}$$

where

$$J(q) = \begin{bmatrix} -L_1 \sin(q_1) - L_2 \sin(q_1 + q_2) & -L_2 \sin(q_1 + q_2) \\ L_1 \cos(q_1) + L_2 \cos(q_1 + q_2) & L_2 \cos(q_1 + q_2) \end{bmatrix}. \tag{15}$$

This Jacobian is utilized to relate motion in joint space to motion in Cartesian space, and forms the basis for the task-space impedance controller introduced in Section 3.

4.3 Task-Space Force Mapping

To implement Cartesian impedance control, the desired virtual end-effector force is mapped to actuator torques through the Jacobian transpose,

$$\tau_{\text{task}} = J(q)^T F. \tag{16}$$

This mapping enables the controller to regulate end-effector motion directly in Cartesian space while producing motor torques that act through the flexible joint dynamics of the system.

4.4 Workspace Considerations

The task is performed close to the manipulator's possible boundary, particularly during contact with the wall and downward sliding motion. In this region, the arm may approach near singular configurations, for example when the second joint angle tends toward full extension. These configurations reduce Jacobian conditioning and may degrade Cartesian tracking performance. Hence, the commanded task space trajectory is limited to remain within a reachable workspace region during simulation.

5 Stability Analysis

5.1 Lyapunov Analysis

To analyse the stability of the closed loop system, a Lyapunov function is defined based on the task space tracking error $\tilde{x} = x_d - x$:

$$V = \frac{1}{2}\dot{\tilde{x}}^T M_d \dot{\tilde{x}} + \frac{1}{2}\tilde{x}^T K_d \tilde{x}, \tag{17}$$

where M_d and K_d are positive definite matrices.

The Cartesian impedance controller imposes second order error dynamics of the form

$$M_d \ddot{\tilde{x}} + D_d \dot{\tilde{x}} + K_d \tilde{x} = 0, \tag{18}$$

where D_d is a positive definite damping matrix.

Differentiating V and substituting the error dynamics gives

$$\dot{V} = -\dot{\tilde{x}}^T D_d \dot{\tilde{x}} \leq 0. \tag{19}$$

This shows that the system dissipates energy over time, and the tracking error converges to zero under such controller.

5.2 Effect of Flexible Joint Damping

Additional damping terms applied at the motor and joint levels,

$$-D_{\text{motor}}\dot{\theta}, \quad -D_\delta \dot{\delta}, \tag{20}$$

further increase energy dissipation and suppress oscillations associated with the flexible joints, improving overall stability.

5.3 Stability in Contact

The impedance controller behaves as a compliant system in task space, allowing controlled interaction with the wall. The combination of stiffness and damping ensures that contact forces remain bounded while preventing instability due to excessive force application.

5.4 Discussion

The Lyapunov-based analysis indicates that the controller results in a dissipative system with stable behaviour in both free motion and contact. Although a full nonlinear proof is not presented, the analysis explains the observed tracking and interaction in simulation.

6 Results and Discussion

6.1 Overall Performance

The controller was evaluated on a wall slide task involving approach, contact, and vertical sliding. The system successfully achieved contact with the wall and maintained a stable sliding motion along the vertical direction.

As shown in Fig. 1, the system exhibits a large transient tracking error followed by gradual convergence. The end-effector successfully reaches the wall and maintains contact while sliding along the vertical direction.

The end-effector tracking error reaches a peak value of 0.77 m during the initial transient phase and decreases to a final value of 0.067 m. The mean tracking error over the full trajectory is 0.215 m.

This indicates that while the controller is stable and convergent, the transient response is relatively large and steady-state accuracy remains imperfect.

6.2 Wall Interaction and Constraint Enforcement

Main design requirement was to limit wall displacement to approximately 10 mm, with any violation considered a failure condition. The results show a maximum displacement of 11.14 mm.

This deviation is small in magnitude but highlights the difficulty of strictly enforcing hard contact constraints in a such control task. The violation is given to a combination of transient impact effects and sustained torque build-up during contact.

Despite this, the system maintained stable interaction with a contact span of approximately 0.022 m, demonstrating successful wall-following behaviour.

6.3 Joint Behaviour

The joint responses show a clear asymmetry between the two joints. Joint 1 exhibits smooth motion with limited oscillation, indicating effective damping and control.

HOwever, Joint 2 displays significant oscillatory behaviour and drift. This is reflected in the final error norms, where the motor-side error reaches 3.05 rad and the link-side error 0.86 rad.

This behaviour is attributed to a combination of flexible joint dynamics, insufficient damping of the elastic mode, and torque build-up during contact. The interaction between posture regulation and contact forces further increases it.

6.4 Torque Response

The torque profiles show that Joint 2 experiences a continuous increase in control effort over time, while Joint 1 stabilises after the initial transient.

This indicates that Joint 2 plays a dominant role in maintaining end-effector posture during contact and is more sensitive to modelling errors and flexible dynamics. The torque build-

up directly contributes to the observed oscillatory behaviour and slight violation of the wall constraint.

6.5 Effect of Control Design

The observed system behaviour is strongly influenced by the control design choices:

- **Cartesian impedance control** ensures compliant interaction with the environment and prevents aggressive contact behaviour.
- **Jacobian transpose mapping** provides a robust and nice force-to-torque mapping, particularly beneficial near singular configurations and during contact.
- **Additional damping terms** (D_{motor}, D_δ) reduce oscillations, although they are insufficient to fully suppress the flexible joint mode in Joint 2.
- **Slow trajectory execution** (35 s duration) reduces excitation of high-frequency dynamics and contributes to overall stability.

The controller parameters were tuned through multiple trial-and-error, with particular emphasis on torque-related gains and damping terms.

6.6 Design Priorities

The primary design objective was to make sure **safe and stable contact** with the wall, rather than achieving high tracking precision. This is reflected in the use of compliant impedance control, conservative force limits, and slow trajectory execution.

As a result, the system achieves robust interaction and avoids aggressive contact, at the expense of larger transient errors and moderate steady-state accuracy.

6.7 Limitations

Despite successful task execution, several limitations are observed:

- Large transient tracking error during the approach phase.
- Significant oscillations and drift in Joint 2 due to flexible joint dynamics.
- Slight violation of the wall displacement constraint (11.14 mm vs 10 mm target).

These limitations suggest that improved damping design or more advanced control strategies may be required for higher precision and stricter constraint enforcement.

6.8 Summary

Overall, the controller achieves good task execution, controlled wall interaction, and successful sliding behaviour. While precision is limited and flexible joint effects remain significant, the system demonstrates strong performance in contact-rich scenarios.

The observed behaviour is good with the stability properties derived in the previous section, where damping ensures energy dissipation and convergence of the task-space error dynamics.

7 Conclusion

The implemented controller demonstrated partial success. In particular, the system successfully had contact with the wall and maintained controlled motion along the vertical direction, achieving approximately 30 mm of sliding as intended.

However, the overall system performance did not reach the desired level of stability and precision. While task-space behaviour appeared stable, significant oscillations were observed in the joint responses, particularly in Joint 2. This indicates that the controller was able to achieve the task at a high level, but struggled to regulate the underlying joint dynamics effectively.

The main limitations are attributed to parameter selection and torque tuning rather than the control structure itself. Although the impedance-based approach provides a suitable framework for compliant interaction, the chosen gains and damping terms were insufficient to fully suppress flexible joint oscillations and torque build-up during contact.

A key part of the system is its ability to maintain safe interaction with the environment while achieving the main objective of wall contact and sliding. This demonstrates that the control strategy is fundamentally appropriate for contact tasks.

Future improvements could focus on better tuning of damping parameters, particularly for the flexible joint modes, as well as refining the overall task execution strategy. .

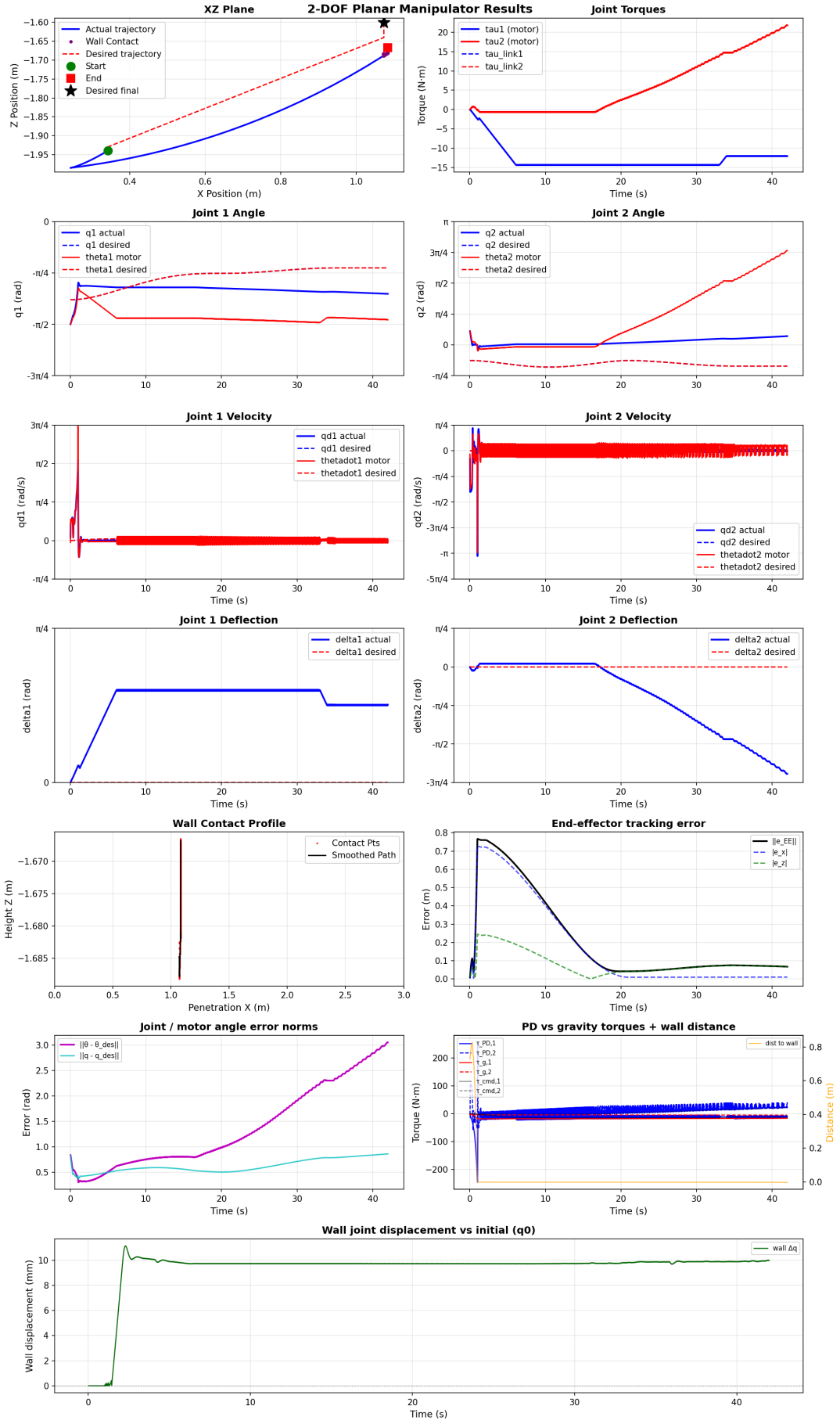

Figure 1: Closed-loop response of the flexible-joint manipulator during task. The system achieves stable contact and bounded wall displacement, while exhibiting large transient tracking error and oscillatory behaviour in Joint 2 due to flexible dynamics.